Supplement of Hydrol. Earth Syst. Sci., 26, 2541–2560, 2022
https://doi.org/10.5194/hess-26-2541-2022-supplement

Hydrology and Earth System Sciences
Open Access

Supplement of

Inclusion of flood diversion canal operation in the H08 hydrological model with a case study from the Chao Phraya River basin: model development and validation

Saritha Padiyedath Gopalan et al.

Correspondence to: Saritha Padiyedath Gopalan (charu666@gmail.com, pgsaritha@nies.go.jp)

S1 Schematic of the canal diversion scheme

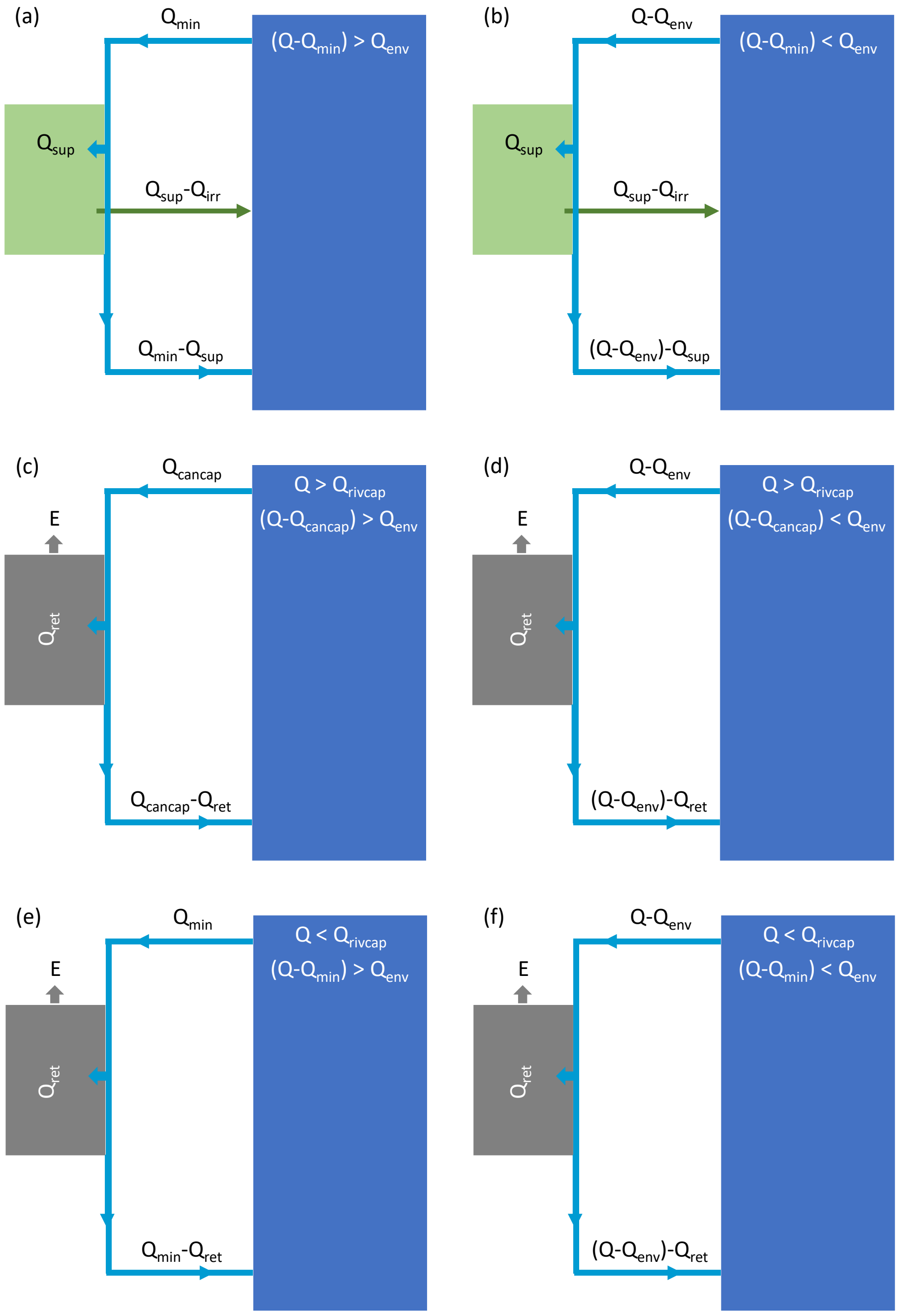

Figure S1: Schematic diagram of the canal diversion scheme during the (a-b) low flow in dry season, (c-d) flood flow in wet season, and (e-f) non-flood flow in wet season. Blue, green, and grey symbols denote river, agricultural land, and retention areas, respectively. Blue and green arrows represent the canal flow and return flow from agricultural land, respectively.

S2 Water infrastructures in the CPRB

S2.1 Canal system

Table S1 shows the observed river channel carrying capacity, canal carrying capacity, and minimum flow of diversion at the origins of the eleven canal systems. Table S1 also shows the simulated values under the regionalized and generalized schemes as explained in section S3.

Table S1. Observed (OBS) and simulated (REG for regionalized and GEN for generalized simulations) values of river channel carrying capacity at the canal origin, canal carrying capacity, and the minimum flow diversion of each canal for the CPRB.

No.	Canal system	River channel carrying capacity (m^3/s)			Canal carrying capacity (m^3/s)			Minimum flow diversion (m^3/s)		
		OBS	REG	GEN	OBS	REG	GEN	OBS	REG	GEN
1	Yom – Nan 1	850	400	284.3	300	300	42.0	10	10	9.2
2	Yom – Nan 2	600	400	414.1	250	250	62.9	10	10	14.0
3	Chainat – Pasak	2000	2500	2356.2	210	210	362.9	100	100	80.9
4	Makham Thao – Uthong	2000	1000	2379.6	35	35	365.8	6	7.5	82.0
5	Tha chin	2000	2000	2382.4	320	320	366.1	40	40	82.0
6	Noi	2000	1500	2384.0	230	230	367.4	55	60	82.6
7	Chainat – Ayutthaya	2000	1000	2393.1	65	65	366.8	15	17	82.1
8	Lopburi	2900	1500	2431.1	150	150	376.5	0	2	85.4
9	Bang Kaeo	2800	1500	2449.0	100	100	380.6	0	0	87.1
10	Phong Pheng	1000	900	2456.7	800	1000	381.2	45	110	87.4
11	Bang Ban	1000	650	2457.6	400	400	383.3	10	25	87.8

S2.2 Reservoirs

Details of the eight multipurpose reservoirs in the CPRB are provided in Table S2. Operation data for all reservoirs were obtained from the Electricity Generating Authority of Thailand (EGAT) and the Royal Irrigation Department (RID), Thailand. For each of the reservoirs, releases during the wet and dry seasons were calculated based on the long-term mean of observed reservoir release data. These long-term mean release values were bias-corrected with respect to simulated inflow because of the difference between observed and simulated inflows into the reservoirs. These bias-corrected releases were then adjusted with reference to reservoir storage targets or limits, which are set based on the upper and lower storage guide curves; these curves critically affect the simulated volume of water stored in the reservoirs. Detailed information regarding the reservoirs and their operation in the CPRB is available from Padiyedath Gopalan et al. (2021) and Mateo et al. (2014).

Table S2. The details of the existing reservoirs in the CPRB (Lehner et al., 2011).

No.	Reservoir	Year of construction	Storage capacity (MCM)	Catchment area (km^2)	Main purposes
1	Mae Ngat	1985	265.0	1281	Irrigation Water supply
2	Mae Kuang	1991	263.0	558	Irrigation Water supply
3	Bhumibol	1964	13462.0	26400	Irrigation Flood control Water supply Hydroelectricity
4	Kiew Lom	1972	112.0	2747	Irrigation Water supply
5	Mae Chang	1983	108.6	290	Water supply Hydroelectricity
6	Sirikit	1974	9510.0	13130	Irrigation Flood control Water supply Hydroelectricity
7	Thap Salao	1988	160.0	531	Irrigation Water supply
8	Pasak	1999	960.0	12970	Irrigation Flood control Water supply

S3 Inclusion of canal systems and retention areas in the H08 model

Eleven canal systems were digitized into the H08 model under the regionalized and generalized schemes, as shown in Fig. S2(b) and (c), respectively. The Chainat-Pasak canal, on the left bank of the Chao Phraya River in the lower CPRB, flows through the Pasak River before emptying into the Gulf of Thailand (Fig. S2a). However, in this study, the Pasak River was regarded as the destination point of the Chainat-Pasak canal because further downstream data were unavailable (Fig. S2b and c).

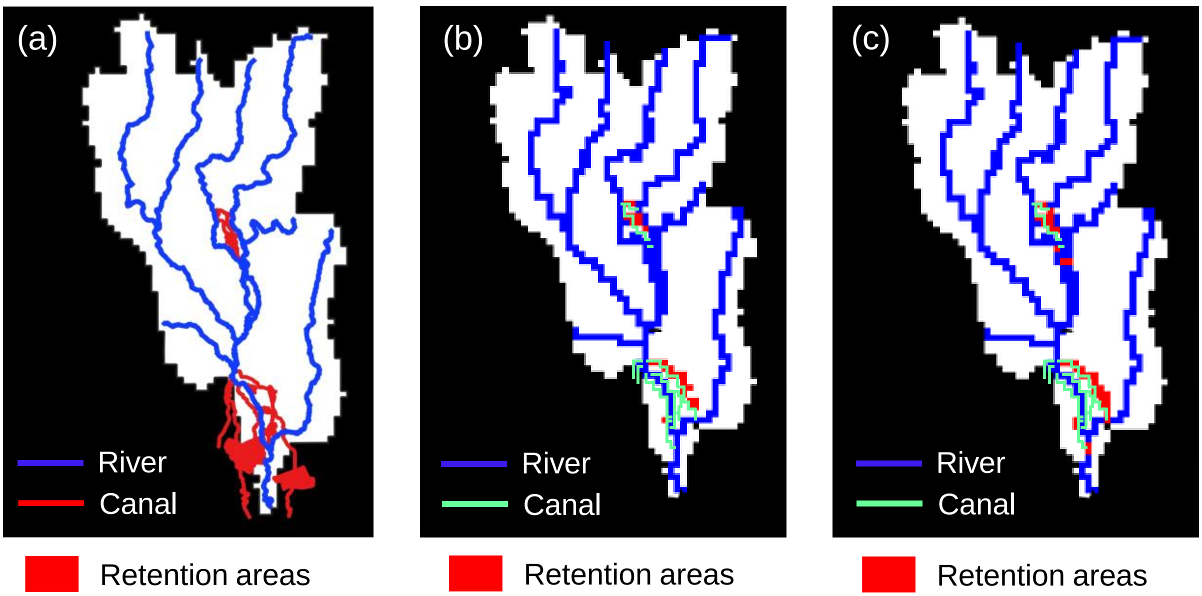

Figure S2: Visual comparison of the canal networks and retentions areas of the CPRB in the (a) observed, (b) regionalized, and (c) generalized canal schemes.

The observed and modeled (regionalized and generalized) areas of the retention ponds associated with each of the canal systems are provided in Table S3. No retention areas were associated with the Yom-Nan 2 and Bang Kaeo canals; retention areas of the Makham Thao-Uthong and Tha Chin canals were excluded from analysis because both the canal and the retention areas lie outside the basin, as shown in Fig. S2(a). The modeled retention areas were smaller in area than the observations for most of the canal systems because there were few rainfed croplands near those networks. The total area of retention ponds was approximately 1702 km^2, whereas the retention areas obtained under the regionalized and generalized schemes were 615 km^2 (approximately one-third of the observed area) and 935 km^2 (approximately half of the observed area), respectively. The small retention areas simulated in the regionalized scheme can be attributed to the refinement of data conducted to match the data provided by the RID.

Table S3. Observed and modelled (regionalized and generalized) areas of the retention areas associated with each canal system.

Basin	Canal system	Observed area (km^2)	Regionalized area (km^2)	Generalized area (km^2)
Upper CPRB	Yom – Nan 1	424.00	276.02	365.96
	Yom – Nan 2	0	0	54.53
Lower CPRB	Chainat – Pasak	250.69	223.07	294.14
	Noi River	780.21	0	14.23
	Chainat – Ayutthaya	27.20	26.40	26.40
	Lopburi	132.8	89.64	154.16
	Bang Kaeo	0	0	0
	Phong Pheng	33.37	0	0
	Bang Ban	53.52	0	25.87
Total		1701.79	615.13	935.29

Before conducting canal simulations, values of variables such as the river channel carrying capacity, canal carrying capacity, and the minimum flow of diversion were set for both canal schemes. In the regionalized scheme, an adjusted version of the observed values of these variables was used for the H08 model because the simulated discharge was slightly lower than the observed discharge at various diversion locations. In the generalized scheme, Q_5, Q_{50}, and Q_{90} values were used to represent river channel carrying capacity, canal carrying capacity, and minimum flow of diversion, respectively.

Fig. S3 is a scatter plot comparing the values of the river channel carrying capacity, canal carrying capacity, and minimum flow of diversion for the regionalized (top panel) and generalized (bottom panel) canal schemes to the observed values. The regionalized estimates exhibited slight variation from the observations because of the adjustment noted above. Under the generalized scheme, the river carrying capacity values were underestimated at the origin of flood diversion canals while overestimated for multi-purpose channels. Although these values exhibited slight variations, they were comparable with the observations, except in two canal systems (Phong Pheng and Bang Ban; Table S1). The low observed river carrying capacity at the origins of these two canal systems is to achieve a maximum discharge reduction at Ayutthaya (C.35 station), where the channel carrying capacity is small. The canal carrying capacity was almost close for most of the canals. Likewise, the minimum flow diversion values for many of the canal systems were similar. This is because of the very small inflow contributions into the lower Chao Phraya River. Their values exhibited deviations with respect to the observations. Most of these deviations were in values for multi-purpose canals, because the primary purpose of all canals under the generalized scheme is flood control. These values were subsequently employed for the canal simulations.

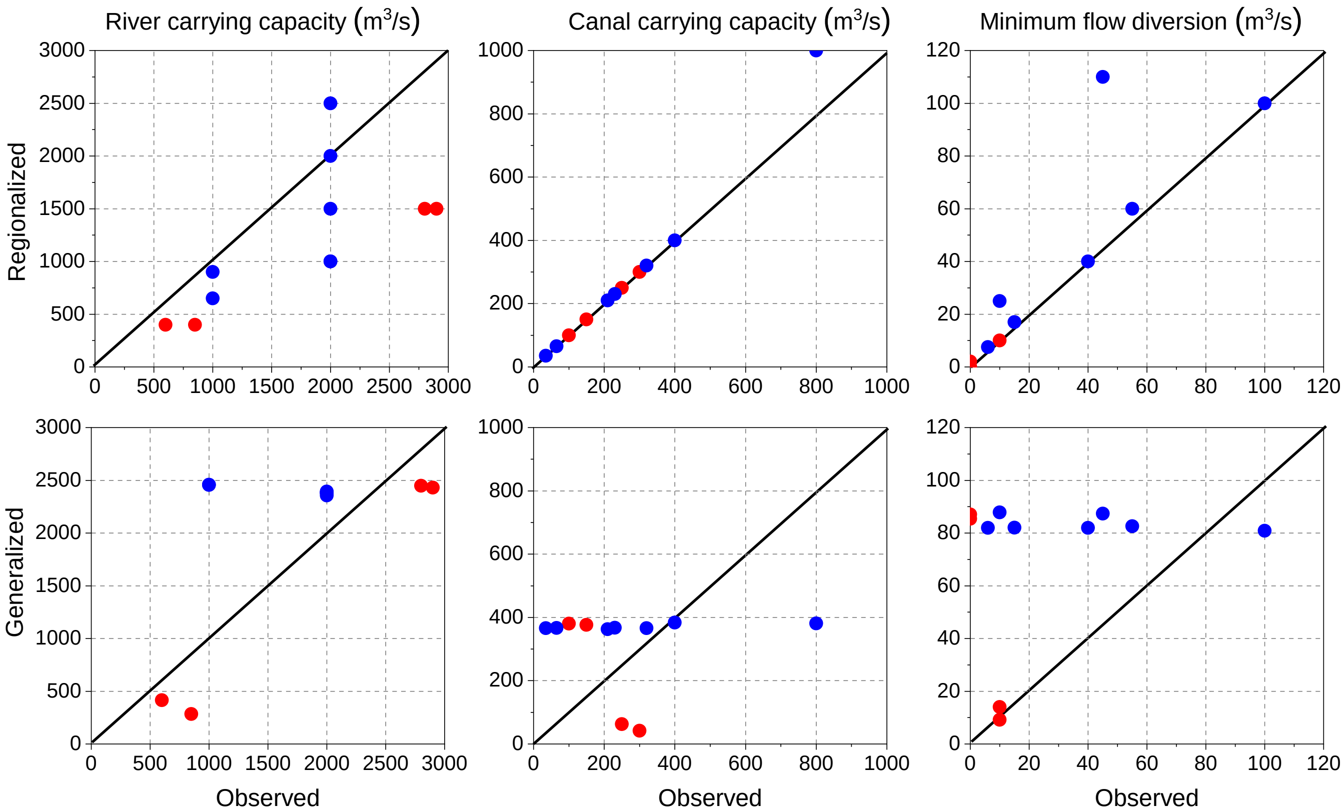

Figure S3: The scatter plot of the observed values of the river carrying capacity, canal carrying capacity, and the minimum flow of diversion against the values of the regionalized and generalized canal schemes. The red and blue circles represent the flood and multi-purpose canal systems, respectively.

S4 H08 model calibration and validation

S4.1 Naturalized discharge simulation

The H08 model was recalibrated at Nakhon Sawan for estimation of naturalized discharge (NAT) because new groundwater components were incorporated into the H08 model (Hanasaki et al., 2018). This recalibration was performed by keeping the remaining settings identical to the settings described by Padiyedath Gopalan et al. (2021). The calibrated parameters of the land surface hydrology module for the CPRB are shown in Table S4, along with the corresponding global parameters. Using these calibrated parameters, the NAT discharge was simulated by enabling the land surface hydrology and river routing modules. These modules do not include the effect of water infrastructures and thereby simulate the NAT discharge. Further, the observed naturalized discharge at Nakhon Sawan was reconstructed by removing the effect of two major dam reservoirs (Bhumibol and Sirikit) operating upstream of the station. This was performed by adding the water stored in the two dam reservoirs with the observed discharge at Nakhon Sawan (Mateo et al., 2014). The transformation of observed discharge into the observed naturalized discharge and the associated uncertainties are described in detail by Champathong et al. (2020). The estimation of the observed naturalized discharge at Nakhon Sawan was carried out using the following equation:

$$Q_{Nat} = Q_{Obs} + [I + P - R - S]_{Bhumibol} + [I + P - R - S]_{Sirikit} \quad \text{(S1)}$$

where Q_{Nat} is the observed naturalized discharge, Q_{Obs} is the observed discharge, I is the reservoir inflow, P is the water pumped into the reservoir, R is the reservoir release, and S is the water released through the spillway. Further, the computed observed naturalized discharge was compared with the simulated NAT discharge from the H08 model to examine the hydrograph reproducibility. Naturalized discharge was adequately reproduced at Nakhon Sawan, with daily and monthly Nash-Sutcliffe efficiency (NSE) values of 75.18% and 86.07%, respectively. Furthermore, the observed and simulated annual average river discharges were 701 and 692 m^3/s, respectively; these differed by only 1.3%.

In addition, model validation was conducted at 28 stations in the CPRB (Fig. 4) using NSE as the evaluation criterion. The minimum and maximum daily NSE values were 31% and 87%, respectively, with a mean value of approximately 49%. Similarly, the monthly NSE values ranged from 33% to 90%, with a mean value of approximately 67%. Overall, the performance of the H08 model was very good at four stations (monthly NSE values of 75−100%), good at thirteen stations (monthly NSE values of 65−75%), and satisfactory at eight stations (monthly NSE values of 50−65%), based on monthly NSE values (Moriasi et al., 2007). However, unsatisfactory performance was observed at three stations located in the far upstream reaches of the river networks; these monthly NSE values were below 50%.

Table S4. Calibrated parameters of land surface hydrology module at Nakhon Sawan.

Parameters	Global setup	Regional setup
Soil depth (m)	1.00	2.50
Bulk transfer coefficient	0.003	0.013
Time constant (day)	100	70
Shape parameter	2.00	2.30
Groundwater depth (m)	1.00	0.50
Groundwater yield	0.30	0.10
Groundwater time constant (day)	2.00	4.00
Groundwater shape parameter	100	50

S4.2 Dam discharge simulation

The ability of the H08 model to explicitly reproduce the observed discharge hydrograph at Nakhon Sawan, using the recalibrated parameters, was evaluated by enabling the reservoir operation module of the H08 model in addition to the land surface hydrology and river routing modules. This will facilitate the comparison of the observed discharge with the simulated dam discharge (DAM) under the assumption that the DAM discharge could act as a proxy for the observed discharge although precisely not the case because the DAM discharge simulation does not include water abstraction for irrigation. Still, this comparison was made to evaluate the performance of the included reservoir operations in the model. Reservoir operation rules were set in accordance with the operation rules described by Padiyedath Gopalan et al. (2021), based on the upper storage guide curves of historical reservoir operation. The model exhibited good performance, with daily and monthly NSE values of 75.61% and 80.75%, respectively. Moreover, the observed and simulated annual average river discharges were 673 and 686 m^3/s, respectively; these differed by only 1.9%.

S4.3 Irrigated discharge simulation

In Asian countries, canal systems serve as floodways during the wet season and water supply channels during the dry season. Hence, estimating irrigation water demand is crucially important in running the simulation over a year. In the H08 model, the crop growth module estimates the crop calendar and associated crop yields. In the coupled model, irrigation water demand and streamflow were utilized to estimate water withdrawal. Therefore, in this section, we validated the simulated crop calendar, crop yields, and irrigation water withdrawal through the comparison of the results obtained here with previous reports and the expert opinions of RID officials in Thailand.

S4.3.1 Crop calendar and yield

Initially, we simulated the crop calendar of different crops using the stand-alone crop growth module of the H08 model. For calculation of the crop calendar, we multi-averaged the variables (air temperature, shortwave downward radiation, evapotranspiration, and potential evapotranspiration) that were used to compute the crop calendar from 1980 to 2004. Then by utilizing these multi-year averaged variables, we estimated a single crop calendar for each of the crops in CPRB. Then, we validated the crop calendar of three major crops in Thailand by comparing the simulated crop calendar with the calendar reported in the agricultural handbook of the World Agricultural Outlook Board, United States Department of Agriculture (WAOB-USDA, 1994), which provides planting and harvesting dates for major crops in countries worldwide. The three selected crops are rice (first and second crop), maize, and sugarcane, as shown in Fig. S4.

Rice is the major crop grown in Thailand, with two main cropping seasons known as the first and second rice crops (Titapiwatanakun, 2012). According to WAOB-USDA (1994), the first rice crop is grown mainly from May to August in most of Thailand, and its harvesting period is from October to January of the following year (Fig. S4). The second rice crop is irrigated and grows in the dry season from January to early March, with harvests from May to June (WAOB-USDA, 1994). Another report by Titapiwatanakun (2012) notes that the first and second rice crops are grown from May to October and November to April, respectively, providing a wide cropping calendar with a span of six months related to regional differences in cropping schedules. Overall, by combining the reports of WAOB-USDA (1994) and Titapiwatanakun (2012), the planting and harvesting dates were adequately reproduced in the simulations for the first and second rice crops, although they exhibited a lag of approximately one month compared with the WAOB-USDA report, as shown in Fig. S4.

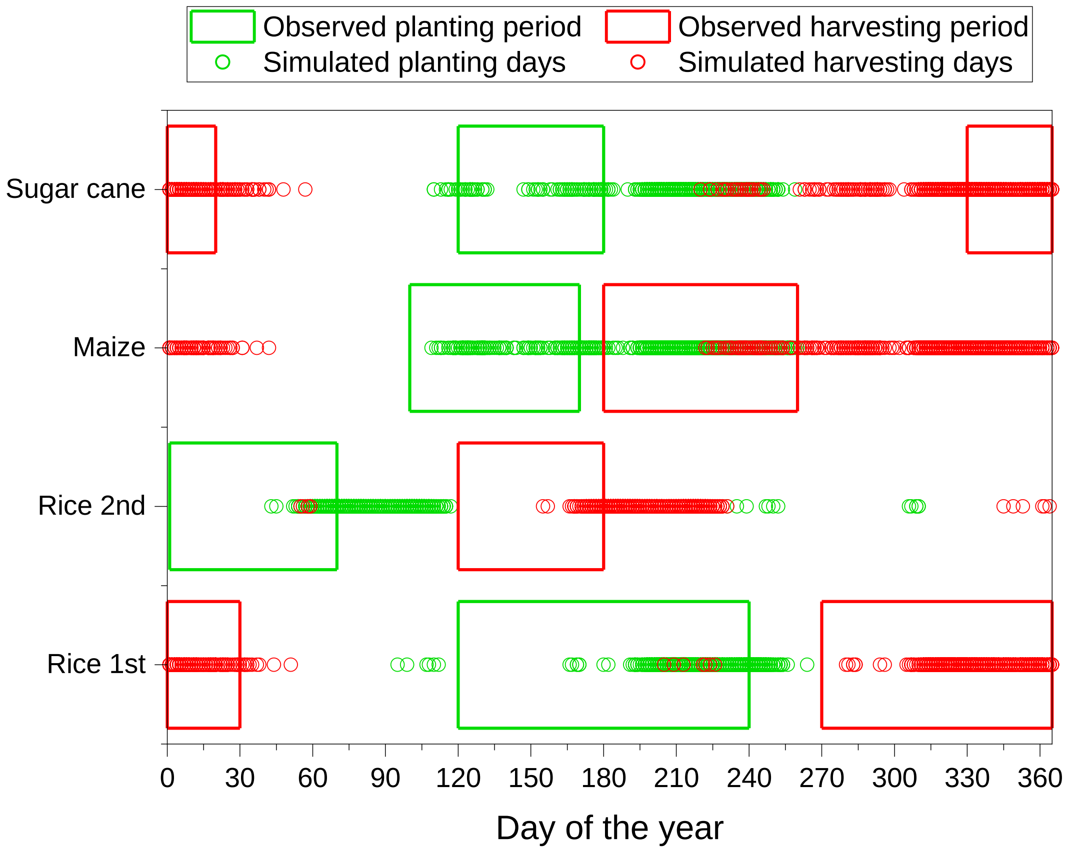

Figure S4: Observed and simulated planting and harvesting dates for rice (first and second crop), maize, and sugarcane. Each circle represents each grid cell in the H08 model domain.

For maize, the simulated planting dates were well reproduced. Although early April to late June is the most suitable planting period for maize, it may be planted from March to September based on soil moisture availability (Senanarong, 1968), which was adequately reflected in the simulations. The simulated planting dates aligned with the observations, but they occurred approximately one month later in some regions. Similar to the planting dates, the harvest dates showed a wide range of up to five months. The simulated planting and harvesting dates were fairly captured for sugarcane in most areas. Some regions showed differences from the observations, reflecting variations in regional conditions. In general, the planting and harvesting dates of major crops in the CPRB closely agreed with the WAOB-USDA data. The exceptions to this tendency included late estimation of both planting and harvest dates by nearly one month, as well as cropping periods longer than the observed data.

Using the simulated crop calendar, we estimated the potential yields of the three major crops and compared the results with yields in the WAOB-USDA report (Fig. S5). The simulated annual average yields of rice (first crop) and maize from 1980 to 2004 were 4–6 t/ha and 8–10 t/ha, respectively. The simulated yields of these crops were high, compared with observed yields of 1.94 t/ha (rice) and 2.76 t/ha (maize). These differences may have arisen for several reasons. First, crop yield was estimated based on heat unit theory, which assumes that the rate of growth is directly proportional to the increase in temperature (Hanasaki et al., 2008). Thailand has a warm climate, causing heat unit theory to slightly overestimate potential yields. Second, the parameters of the crop module were set according to US standards; these values will differ for Asian countries. Third, no fertilizer stress was applied to the crops in the model. Conversely, the simulated yield of sugarcane was 4–8 t/ha, which was smaller than the observed value of 47.77 t/ha. This difference is presumably because the WAOB-USDA report does not separate yields into irrigated and non-irrigated, while most sugarcane cultivation in Thailand is rainfed. Although the crop growth module of the H08 model predicts crop yields, it was designed primarily for simulating crop calendars. This further amplified the fluctuations in predicted yield.

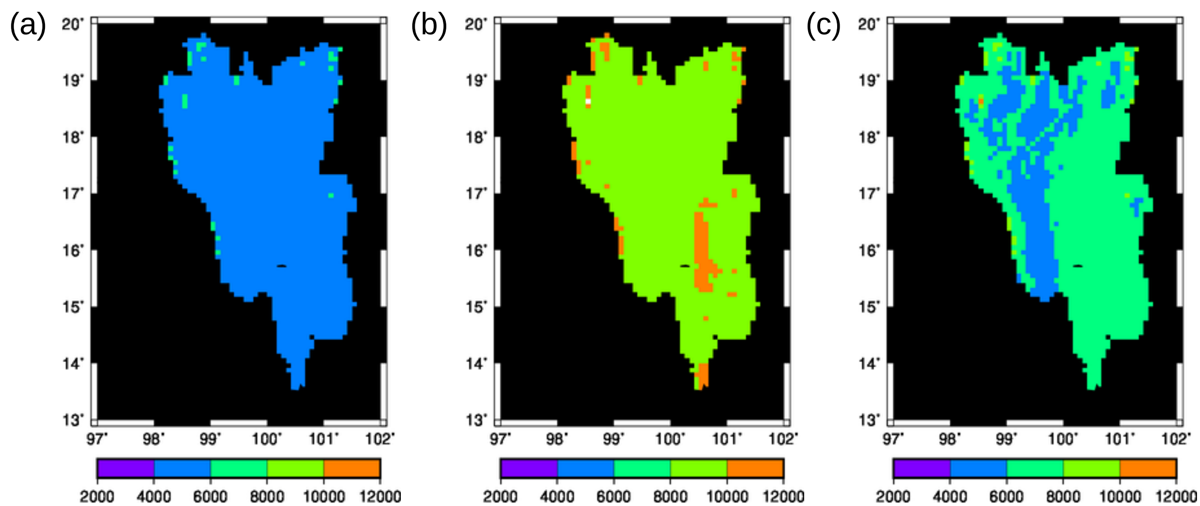

Figure S5. The simulated annual average yield of the major crops, (a) rice, (b) maize, and (c) sugarcane in kg/ha.

S4.3.2 Irrigation water withdrawal

The coupled H08 model simulates irrigation water withdrawal based on consumptive water use and regional irrigation efficiency. The irrigation efficiency and cropping intensity for the CPRB were set to 50% and 1.5, respectively (Molle et al., 2001; FAO, 2013). Irrigation efficiency of 50% indicates that approximately 50% of the water withdrawn for irrigation becomes delivery losses and return flow. Cropping intensity of 1.5 means that on average 150% of the total irrigated cropland is used for cultivation. Reported irrigation water withdrawal for Thailand is approximately 51.8 km^3/year (FAO 2013; Kiguchi et al., 2021), of which nearly 75% (38.9 km^3/year) is utilized in the CPRB based on the Water Resources Master Plan produced by the Office of the National Water Resources. Furthermore, four irrigation simulations were conducted (Table S5) to estimate irrigation water withdrawal in the CPRB in which the virtual inexhaustible and non-renewable water sources were considered in the H08 model to fully meet agricultural water demand and avoid water stress (Hanasaki et al., 2018). Four parameters were used in these simulations (Table S5), representing soil moisture targets for paddy and non-paddy crops. Above this soil moisture threshold, the model assumes no water stress; below this threshold, water stress prevents optimal growth and crop yield (Hanasaki et al., 2008).

Case 1 employed the default parameter values established for the global setup, and the simulated water withdrawal under Case 1 was approximately 74 km^3/year. The parameters were slightly adjusted for three additional cases (Case 2, Case 3, and Case 4) to obtain simulated irrigation water withdrawal comparable with the observation (38.9 km^3/year). In Case 2, irrigation for non-paddy crops was removed, because paddy is the major irrigated crop in Thailand. However, irrigation water withdrawal remained high, with a value of 51.8 km^3/year. The soil moisture target for first paddy crops (rainy-season crops; Fig. S4) was reduced to 0.9 in Case 3, and the simulated water withdrawal (33.7 km^3/year) was comparable with the observation. For Case 4, the soil moisture target was further reduced to 0.8 for the first paddy crops, while full irrigation was maintained for the second crops (dry-season crops; Fig. S4). This simulation generated lower irrigation water withdrawal (26.2 km^3/year), compared with the observed data.

Table S5. Validation of the irrigation water withdrawal for the CPRB.

	Simulations	Case 1	Case 2	Case 3	Case 4
Parameters of crop growth module	Factor for paddy (1st crop)	1.0	1.0	0.9	0.8
	Factor for paddy (2nd crop)	1.0	1.0	1.0	1.0
	Factor for non-paddy (1st crop)	0.75	0	0	0
	Factor for non-paddy (2nd crop)	0.75	0	0	0
Simulated irrigation water withdrawal (km^3/year)		74.07	51.78	33.71	26.17

The parameters obtained from all four cases were used to simulate irrigated discharge (IRG) by coupling all six modules of the H08 model. In reality, this IRG discharge should correspond to the observed discharge because it includes most of the human interactions such as the reservoir operation and irrigation water abstraction. Therefore, the IRG discharge was compared with the observed discharge at Nakhon Sawan (C.2 station), the calibration point for the CPRB in this study, for final hydrograph reproducibility. The first three cases were later discarded, and Case 4 parameters were employed for further irrigation simulations, because they best reproduced the observed discharge hydrograph at Nakhon Sawan, as shown in Fig. S6. Irrigation water withdrawal in the CPRB for Case 4 was approximately 50% of the reported irrigation water withdrawal for Thailand; this was acceptable for use in further simulations because specific water withdrawal information was unavailable for the CPRB. The model performed adequately in replicating the observed discharge under Case 4, except for the peak discharge values. The daily and monthly NSE values of the IRG discharge simulation at Nakhon Sawan were 61.93% and 64.58%, respectively.

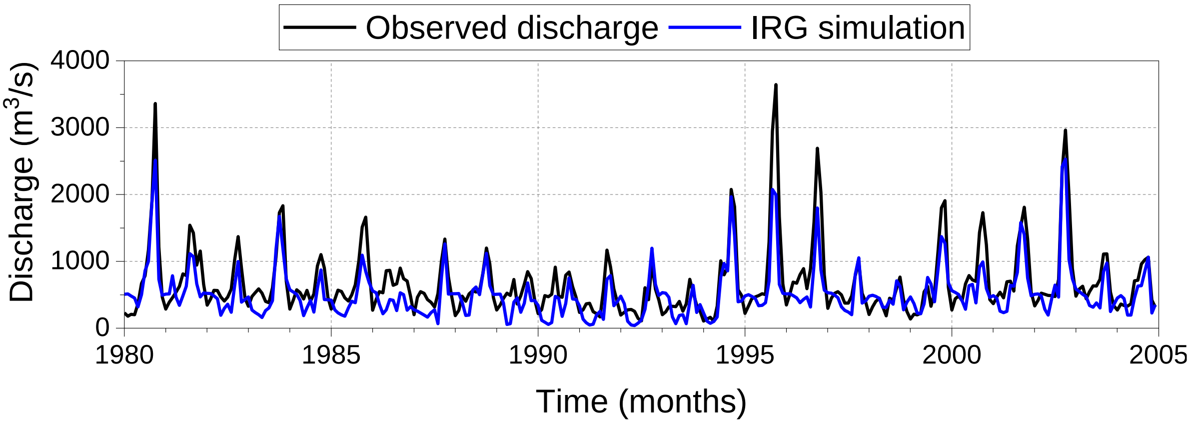

Figure S6: Monthly hydrograph of IRG simulation compared with observed discharge at Nakhon Sawan.

References

Champathong, A., Hanasaki, H., Kiguchi, M. and Oki, T.: Reconstructing the pristine flow of highly developed rivers − a case study on the Chao Phraya River, Hydrol. Res. Lett., 14(2), 89-96. https://doi.org/10.3178/hrl.14.89, 2020.

FAO (Food and Agriculture Organization): AQUASTAT Core Database. Food and Agriculture Organization of the United Nations. http://www.fao.org/aquastat/en/, Database accessed on 2021/04/19, 2013.

Hanasaki, N., Kanae, S., Oki, T., Masuda, K., Motoya, K., Shirakawa, N., Shen, Y., and Tanaka, K.: An integrated model for the assessment of global water resources—Part 1: Model description and input meteorological forcing, Hydrol. Earth Syst. Sci., 12, 1007–1025, https://doi.org/10.5194/hess-12-1007-2008, 2008.

Hanasaki, N., Yoshikawa, S., Pokhrel, Y. and Kanae, S.: A global hydrological simulation to specify the sources of water used by humans, Hydrol. Earth Syst. Sci., 22(1), 789–817, https://doi.org/10.5194/hess-22-789-2018, 2018.

Kiguchi, M., Takata, K., Hanasaki, N., Archevarahuprok, B., Champathong, A., Ikoma, E., Jaikaeo, C., Kaewrueng, S., Kanae, S., Kazama, S., Kuraji, K., Matsumoto, K., Nakamura, S., Nguyen-Le, D., Noda, K., Piamsa-Nga, N., Raksapatcharawong, M., Rangsiwanichpong, P., Ritphring, S., Shirakawa, H., Somphong, C., Srisutham, M., Suanburi, D., Suanpaga, W., Tebakari, T., Trisurat, Y., Udo, K., Wongsa, S., Yamada, T., Yoshida, K., Kiatiwat, T. and Oki, T.: A review of climate-change impact and adaptation studies for the water sector in Thailand, Environ. Res. Lett., 16(2), 023004, https://doi.org/10.1088/1748-9326/abce80, 2021.

Lehner, B., Liermann, C. R., Revenga, C., Vörösmarty, C., Fekete, B., Crouzet, P., Döll, P., Endejan, M., Frenken, K., Magome, J., Nilsson, C., Robertson, J. C., Rödel, R., Sindorf, N. and Wisser, D.: High resolution mapping of global reservoirs and dams and their impact on downstream rivers, Front. Ecol. Environ., 9(9), 494–502, https://doi.org/10.1890/100125, 2011.

Mateo, C. M., Hanasaki, N., Komori, D., Tanaka, K., Kiguchi, M., Champathong, A., Sukhapunnaphan, T., Yamazaki, D. and Oki, T.: Assessing the impacts of reservoir operation to floodplain inundation by combining hydrological, reservoir management, and hydrodynamic models, Water Resour. Res., 50(9), 7245–7266, https://doi.org/10.1002/2013WR014845, 2014.

Molle, F., Chompadist, C., Srijantr, T. and Keawkulaya, J.: Dry-season water allocation and management in the Chao Phraya Delta, DORAS-DELTA: research report, DORAS Center, Kasetsart University, 278 pp., 2001.

Moriasi, D. N., Arnold, J. G., Van Liew, M. W., Bingner, R. L., Harmel, R. D. and Veith, T. L.: Model Evaluation Guidelines for Systematic Quantification of Accuracy in Watershed Simulations, Trans. ASABE, 50(3), 885–900, https://doi.org/10.13031/2013.23153, 2007.

Padiyedath Gopalan, S., Hanasaki, N., Champathong, A. and Tebakari, T.: Impact assessment of reservoir operation in the context of climate change adaptation in the Chao Phraya River basin, Hydrol. Process., 35(1), e14005, https://doi.org/10.1002/hyp.14005, 2021.

Senanarong, A.: Problems of Maize Cultivation in Thailand, Tropical agriculture research series: proceedings of a symposium on tropical agriculture researches, Japan International Research Center for Agricultural Sciences, ISSN: 03889386, 65-70, https://www.jircas.go.jp/en/publication/tars/2/65, (Accessed 28 April 2021),1968.

Titapiwatanakun, B.: The rice situation in Thailand, Support for the Association of Southeast Asian Nations Plus Three Integrated Food Security Framework: Technical Assistance Consultant's Report, Asian Development Bank, Available from: https://www.adb.org/sites/default/files/project-document/73083/43430-012-reg-tacr-04.pdf (Accessed 28 April 2021), 2012.

WAOB-USDA (World Agricultural Outlook Board US Department of Agriculture): Major world crop areas and climatic profile, US Department of Agriculture, Washington DC, USA, 1994.